J. Fluid Mech. (2000), *vol.* 414, *pp.* 367–378. Printed in the United Kingdom

Drop formation behaviour of a hydrate-forming liquid in a water stream

By MASAHIRO KATO†, TOMOYUKI IIDA‡ AND YASUHIKO H. MORI¶

Department of Mechanical Engineering, Keio University, 3-14-1 Hiyoshi, Kohoku-ku, Yokohama 223-8522, Japan

(Received 1 September 1999 and in revised form 11 January 2000)

Experiments were carried out to investigate the drop formation behaviour of a hydrophobic hydrate-forming liquid, HCFC-141b (CH_3CCl_2F), at a single nozzle in a water stream under hydrate-formable thermodynamic conditions. Attention was focused on the relation between the clathrate-hydrate formation and the drop formation. It was observed that two discrete hydrate crusts grow along the liquid–liquid interface; one forms a frontal cap and the other forms a cylindrical root on each growing drop before its detachment from the nozzle. Most of the latter crust remains at the tip of the nozzle after the detachment of the drop so that it grows into a bell-shaped or nearly cylindrical funnel composed of hydrate deposits in the course of successive growth/detachment of drops. The size of these drops is dependent on the instantaneous diameter of the hydrate-funnel tip rather than the diameter of the nozzle itself. Thus, the size of the drops successively released into the water stream generally varies synchronously with quasi-periodical alternation of growth and breaking of the hydrate funnels. The growth and breaking of the hydrate funnels and the resultant drop-size variation are significantly dependent on the system temperature (or the system subcooling from the liquid/liquid/hydrate equilibrium temperature), the nozzle diameter, and the velocity of the drop-forming liquid through the nozzle.

1. Introduction

Clathrate hydrates (abbreviated to 'hydrates' hereafter) are crystalline compounds formed by water molecules (*host* molecules) hydrogen-bonded into a structure of interlinked cages, each enclosing at most one molecule (*guest* molecule) of some apolar substance. The substances that could serve as guest molecules under appropriate thermodynamic conditions are referred to as hydrate formers or guest substances. Numerous substances are known as hydrate formers. Under relevant hydrate-formable thermodynamic conditions, most are liquids or gases immiscible with water. Once a hydrate former immiscible with water is brought into contact with a water phase under appropriate thermodynamic conditions, the formation and growth of the hydrate occur most probably at the interface between the hydrate-former and the water phases.

In this study, we focused on the hydrate formation caused by steady issuing of a liquid hydrate former into water through a nozzle. The interaction between the

† Present address: Mie Factory, Fuji Electric Co., Ltd., Yokkaichi-shi 510-0013, Japan.
‡ Present address: Power Plant Division, Kawasaki Heavy Industries, Ltd., Tokyo 136-0072, Japan.
¶ Author to whom correspondence should be addressed: e-mail yhmori@mech.keio.ac.jp.

hydrate formation and drop formation is of particular interest. This subject has relevance to some technologies which may be realized in the future. For example, cool energy storage systems for domestic air conditioning may be so designed that a liquid hydrate former is directly injected into a water pool, resulting in the formation and storage of hydrate crystals which will be suspended or sedimented in the pool. For direct disposal of CO_2 captured from power-plant flue gases in the ocean at depths of 500–2000 m (an option for CO_2 disposal/storage scenarios to mitigate CO_2 emissions into the atmosphere), pressurized liquid CO_2 may be released into the sea from fine orifices drilled in a long pipe trailed by a CO_2 tanker (Ribeiro & Henry 1995; Fujioka *et al.* 1997). Because of the low temperatures (2–7 °C) and high pressures at the depths of the CO_2 release, CO_2 hydrate will form at the CO_2–seawater interface extending from each orifice into the sea.

Up to now, some fragmentary observations of liquid-CO_2 injection into water under hydrate-formable conditions have been reported by several research groups such as Aya, Yamane & Yamada (1992), Ozaki *et al.* (1992), and Hirai *et al.* (1995). These observations were made exclusively on short-time injection of liquid CO_2 from single nozzles, and hence they do not necessarily represent the situation of steady issuing of a hydrate former into water. To our knowledge the only observation of longer-term (not always steady) issuing of a hydrate-forming liquid reported so far is that on the sea floor at 1335–1550 m depth in a hydrothermal field in the mid-Okinawa Trough by Sakai *et al.* (1990). This showed the emerging of a CO_2-rich liquid out from the seafloor, causing the formation of hydrate chimneys through which the CO_2-rich liquid flowed out into the sea, turning into discrete drops.

The present study aims to investigate experimentally the behaviour of drop formation, possibly interacting with hydrate formation, under conditions in which a hydrate-forming liquid is steadily supplied to a nozzle submerged in a medium of temperature-controlled water. The flow velocity of the hydrate-forming liquid in the nozzle is kept below the so-called jetting velocity so that drops would detach directly from the nozzle tip in the absence of any effect of hydrate formation.

2. Experiments

The experiments were so designed that 1,1-dichloro-1-fluoroethane (CH_3CCl_2F), a hydrochlorofluorocarbon (HCFC) refrigerant known as R-141b, was supplied at a prescribed flow rate to a tubular nozzle held vertically, with its tip facing downward, in a vertical downward flow of water. The selection of R-141b as the hydrate- and drop-forming liquid was for experimental convenience, since it is in the liquid state at room temperature at atmospheric pressure ($\sim$101 kPa), and it can react with water to form a hydrate of structure II at temperatures lower than 8.4 °C at pressures exceeding $\sim$42 kPa (Akiya *et al.* 1991; Brouwer *et al.* 1997). Taking advantage of this, we conceived experiments exclusively at atmospheric pressure, which made our construction of an experimental setup much easier. Each liquid was adjusted in advance to the same temperature, lower than 8.4 °C, and then they were brought into contact. To remove the heat released by the hydrate formation and thereby to maintain the system temperature uniform and constant, the water flow was held steady, unidirectional around the R-141b flow.

2.1. *Apparatus*

The apparatus we constructed was composed of a closed water loop and a one-way R-141 flow, which met in a test column to form R-141b drops and R-141b hydrate

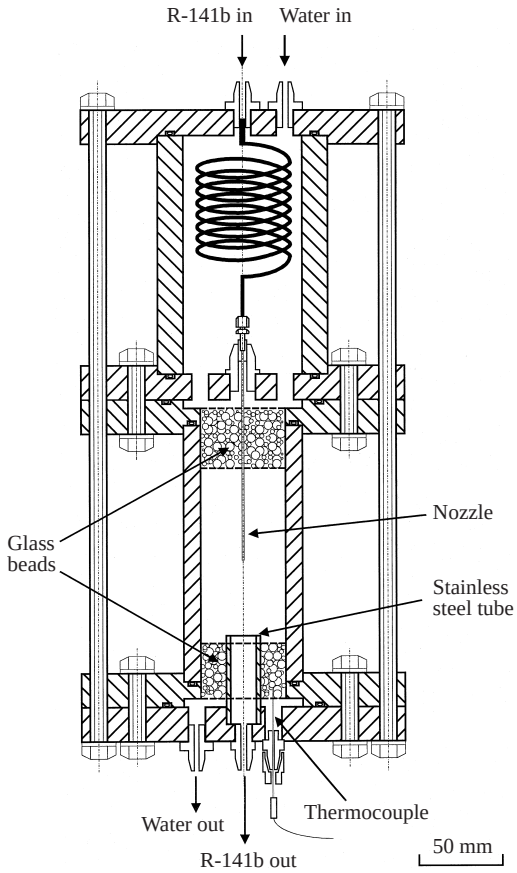

FIGURE 1. Vertical cross-sectional view of the major portion of the apparatus – an assembly of the test column (the lower portion) and an R-141b–water heat exchanger (the upper portion). Water and R-141b, individually temperature-controlled, flow into the heat exchanger to minimize the temperature difference between them in advance of flowing into the test column, wherein R-141b issues into a water stream.

in a water stream. Figure 1 illustrates the structure of the test column (the lower part) and an R-141b–water heat exchanger (the upper part). Water and R-141b, individually temperature-controlled, were supplied to the heat exchanger to minimize the temperature difference between them before flowing into the test column, wherein R-141b issued into a water stream. The test column was made of a transparent PMMA (poly(methyl methacrylate)) cylinder, 50 mm in inside diameter. Its top and bottom portions, each 25 mm in height, were packed with 3.5 mm diameter glass beads in stainless-steel nets to ensure that the water stream has a nearly uniform flow in most of the test column. The water from the bottom glass-bead layer was circulated through an integrated cooler/pump device (Model UC-65 manufactured by Tokyo Rikakikai Co., Tokyo), a needle valve and a flow meter, and then returned to the heat exchanger at the top of the test column.

R-141b was stored in a stainless steel syringe-infusion pump equipped with a cooling-water jacket (High-Pressure Microfeeder Model JP-H manufactured by Furue Science Co., Tokyo). After flowing through the helical stainless steel tube in the heat exchanger, R-141b flowed into a straight stainless-steel tubular nozzle. The nozzle was

130 mm long and was inserted into the test column such that its tip was located at the centre of the column. Three nozzles of 0.6, 1.0 and 3.0 mm inside diameter D_N were used. Every nozzle had the tip sharply cut at right angles. R-141b issued from the nozzle into the water stream in the form of drops, then fell into a stainless-steel tube, 17 mm in inside diameter, immersed in the bottom glass-bead layer, and flowed out of the test column. A small amount of circulating water was also drained from the test column through this outlet. The water was separated from the R-141b effluence in a gravitational separator and sent to the cooler/pump device to join the main water-circulation loop.

The test column and the heat exchanger illustrated in figure 1 were immersed in a rectangular water bath made of transparent PMMA plates. The cooling water, temperature controlled and pumped by the second cooler/pump device, was circulated through this bath and the cooling-water jacket of the syringe-infusion pump storing the R-141 sample. The role of the water bath was to minimize both the temperature fluctuation inside the test column and the optical distortion due to the curvature of the cylindrical PMMA wall of the test column.

2.2. *Procedure*

The procedure for starting up the apparatus for each set of experiments was rather complicated; it included many steps for completely evacuating the liquid flow loops and then filling them with the test liquids. These steps, which were crucial to keep the flow loops free from air bubbles and to ensure stable experimental operations, are detailed elsewhere (Kato 1998). We note here that we used an artificial trigger for hydrate nucleation in the test column to start up each experimental run to eliminate the induction time for spontaneous nucleation of R-141b hydrate, which may be very long even at temperatures well below 8.4 °C, the hydrate/water/R-141b equilibrium temperature. An R-141b hydrate slurry was formed in advance in an external crystallizer filled with a water-rich immiscible mixture of R-141b and water by cooling and agitating the mixture. A small amount of the slurry was injected into the cooler/pump device in the water-circulation loop so that hydrate particles contacted the surface of an R-141b drop pendent from the nozzle tip in the test column, causing the growth of a hydrate film on the drop surface. Once this occurred, the apparently periodical growth and breaking off of the hydrate phase took place at the R-141b/water interface extending from the nozzle tip, synchronously with the successive R-141b drop detachment.

Throughout the experiments reported in this paper, the water flow rate was held constant such that the apparent velocity of water in the test column was 26 mm s^{-1}. The flow velocity of R-141b through the nozzle, V_N, was adjusted to a prescribed level in the range from 10 to 145 mm s^{-1}. Even the highest velocity tested, i.e. 145 mm s^{-1} in the nozzle of 1.0 mm i.d., was well below the jetting velocity relevant to the experimental system. The temperature inside the test column, T, was controlled within ± 0.3 K about a prescribed level (1.0 °C, 3.0 °C or 6.0 °C) during each experimental run.

The hydrate growth and drop formation were recorded using an Olympus SZ-45TR stereomicroscope connected to a Sony CCD-IRIS/RGB video camera. The view axis was held horizontal under diffusive back-lighting of the test column. The video-recording in each run was started just before performing the artificial hydrate-nucleation procedure described above and was continued for 40–200 min.

	R-141b	Water
Density ρ(kg m^{-3})	1275[a]	999.9[b]
Viscosity η(Pa s^{-1})	0.540×10^{-3}[c]	1.731×10^{-3}[b]
Interfacial tension σ(N m^{-1})	$(33.5 \pm 1.4) \times 10^{-3}$[d]	

TABLE 1. Physical properties of R-141, water and their interface: (*a*) saturated liquid at 1 °C (JAR 1994), (*b*) compressed liquid at 1 °C under atmospheric pressure (PROPATH Group 1990), (*c*) saturated liquid at 1 °C (Kumagai & Takahashi 1993), and (*d*) compressed liquids at 9.2 °C under atmospheric pressure (Ohmura *et al.* 2000).

2.3. *Materials in relation to experimental conditions*

The R-141b liquid we used was a commercial refrigerant of 99.9 wt% certified purity (Daikin Kogyo Co., Osaka, Japan). Each experimental run was carried out with a prescribed volume (about 400 cm^3) of fresh R-141b liquid poured into the syringe-infusion pump just before the run. The liquid drained from the test column was never used again.

The water in the closed water loop was deionized and distilled. Because the water was being recirculated during each experimental run, the concentration of R-141b dissolved in the water stream passing through the test column changed with time. Because hydrate crystals in water in which the relevant hydrate former is not dissolved to saturation dissociate at a rate dependent on the degree of undersaturation (Sugaya & Mori 1996; Mori & Mochizuki 1997), the change in R-141b concentration in the water stream could in principle have some effect on the process of hydrate/drop formation in the test column. However, the volume of water circulated in the loop was several litres, and hence we take the R-141b concentration in the water stream to be constant, throughout each experimental run, at a level much lower than that of saturation. The present experiments are consistent in this respect with the hydrate-growth observations by Ohmura *et al.* (1999) on R-141b drops held stationary in a pool of water not presaturated with R-141b.

Table 1 gives some physical properties of the R-141b–water system, which are considered to be relevant to the drop formation behaviour discussed later. The liquid–liquid interfacial tension was obtained at a temperature slightly exceeding the hydrate/water/R-141b equilibrium temperature. In the (metastable) absence of hydrate, the interfacial tension would probably have slightly higher values in the temperature range covered in the present experiments, 1.0 °C–6.0 °C. The interfacial tension could be further raised as the result of enhanced clustering of water molecules adjacent to the interface due to the prior experience of the interface region with hydrate formation/dissociation. Nevertheless, recent measurements of interfacial tension in an R-141b/water system (Ohmura, Shigetomi & Mori 2000) showed no appreciable change in the interfacial tension in the course of repetition of hydrate formation/dissociation. Thus, we believe that the interfacial tension that actually occurred in the present experiments is reasonably well approximated by the value in table 1.

The drop formation accompanied by hydrate formation must depend not only on the fluid properties in table 1 but also on some mechanical properties, such as the Young's modulus, the yield stress, etc., of the R-141b hydrate. However, no quantitative data are available at present on such properties, although a first effort to investigate the elastic or elastoplastic nature of hydrate films was made very recently (Ohmura & Mori 1998).

D_N(m)	V_N(m s^{-1})	Ca_N	Eo_N	We_N	We_N^*
0.6×10^{-3}	20×10^{-3}	1.03×10^{-3}	0.029	0.0091	0.0041
1.0×10^{-3}	10×10^{-3}	0.52×10^{-3}	0.080	0.0038	0.0017
1.0×10^{-3}	20×10^{-3}	1.03×10^{-3}	0.080	0.0152	0.0068
1.0×10^{-3}	38×10^{-3}	1.96×10^{-3}	0.080	0.0550	0.0245
1.0×10^{-3}	91×10^{-3}	4.70×10^{-3}	0.080	0.315	0.141
1.0×10^{-3}	145×10^{-3}	7.49×10^{-3}	0.080	0.800	0.357
3.0×10^{-3}	20×10^{-3}	1.03×10^{-3}	0.724	0.0457	0.0204

TABLE 2. Hydrodynamic parameters for drop formation set in the experiments. In calculating the dimensionless parameters, the values of physical properties given in table 1 were used despite an inconsistency in the temperature at which each of the properties was evaluated.

2.4. *Hydrodynamic parameters for drop formation*

The parameters directly related to the hydrodynamics of drop formation in the experiments were D_N and V_N. Table 2 lists seven different pairs of D_N and V_N values used in the experiments. Based on conventional hydrodynamic models of drop formation in the absence of any crystallization process (Mori & Mochizuki 1992; Steiner & Hartland 1983), we can list several dimensionless groups each incorporating D_N and/or V_N with some of the physical properties given in table 1 and thereby characterizing an aspect of drop-formation mechanics: the nozzle capillary number $Ca_N(= \eta_c V_N/\sigma)$, the nozzle Eötvös (or Bond) number $Eo_N(= (\rho_d - \rho_c)gD_N^2/\sigma)$, and the nozzle Weber number defined in two different ways, $We_N(= \rho_d D_N V_N^2/\sigma)$ and $We_N^*(= (\rho_c + \rho_d)D_N V_N^2/4\sigma)$, where the subscripts c and d refer to the continuous phase (water) and the dispersed phase (R-141b), respectively, and g is the acceleration due to gravity. The values of these dimensionless groups relevant to each D_N–V_N pair are given in table 2 for reference.

3. Qualitative observations – formation of a hydrate funnel

Once hydrate formation started on the surface of an R-141b drop growing at the nozzle tip, all succesive drops formed were inevitably accompanied by hydrate formation on their surfaces, caused by the formation of a durable hydrate funnel extending from the nozzle tip. How such a hydrate funnel survives one cycle of drop formation may be seen in the two sequences shown in figure 2. These sequences were taken in the same experimental run: (*a*) about 20 min after the onset of hydrate formation and (*b*) after about 80 min. In (*a*), the hydrate funnel is still short. The detachment of a drop tears the funnel to pieces hanging from the nozzle tip (see the first picture). As the next drop grows, some hydrate fragments detached from the funnel move to the apex of the drop and coalesce with each other into the form of a frontal cap, which continues to grow. At the same time, the funnel re-forms into a bell shape with a rigid appearance. The *necking* of the drop leading to its detachment (the rightmost picture) tears the funnel again; a relatively small, frontal part of the funnel is carried away by the drop, while the residual part is left on the nozzle tip. In the course of the repetition of this drop formation/detachment, the hydrate funnel increases its *basic* size, the size of the *root* portion of the funnel not carried away by the drops on detachment. In (*b*), we see a hydrate funnel grown into the form of a *triton* (or *conch*) even just after the detachment of a drop. Clearly, the size of drops

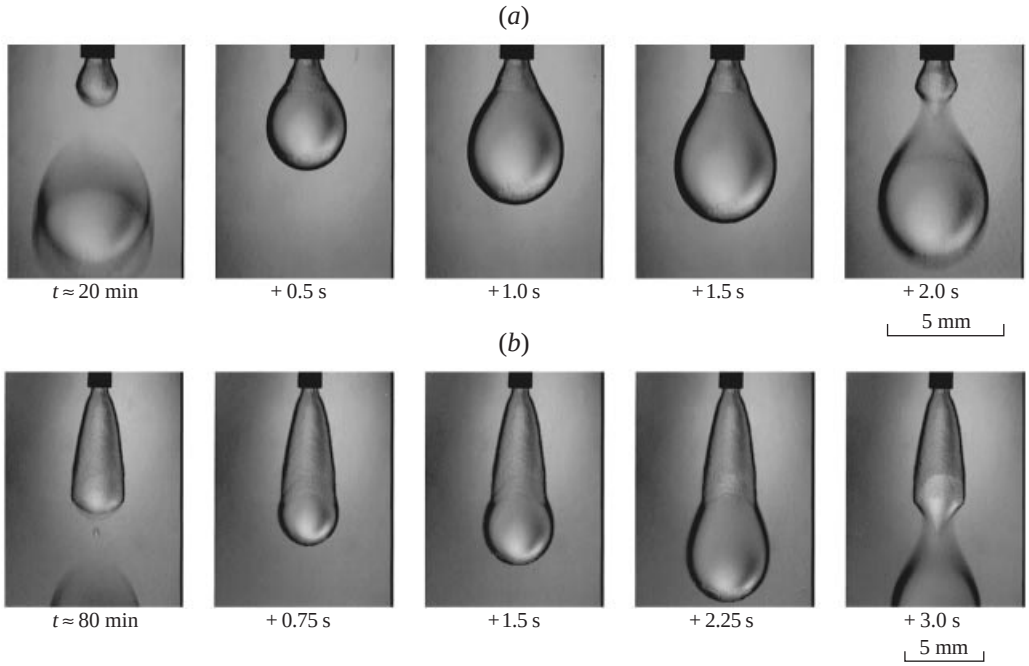

FIGURE 2. Two sequences, (*a*) and (*b*), each showing almost one cycle of the growth and detachment of R-141b drops into the downward flow of water at an apparent velocity of 26 mm s^{-1}. The time lapse t after the hydrate nucleation is shown under the first picture, while the subsequent time lapses are indicated below the other pictures. Both sequences were obtained in the same experimental run in which $T = 1.0\,^{\circ}\mathrm{C}$, $D_N = 1.0$ mm, and $V_N = 38$ mm s^{-1}.

detaching successively is directly related to the instantaneous diameter of the opening of the hydrate funnel rather than to the nozzle diameter.

The pictures in figure 2 suggest that the hydrate films making funnels are rather thin. Although we have no quantitative information, it may be worth estimating, even roughly, the possible order of their thickness. Sugaya & Mori (1996) measured the quasi-steady thickness of a hydrate film formed at the interface between water and a hydrate-forming hydrofluorocarbon liquid, R-134a (CF_3CH_2F), both held stationary, to be $\sim 10\,\mu$m. They assumed that this quasi-steady thickness is obtained when the rate of hydrate-crystal dissociation on the water side of the film and the rate of hydrate-crystal formation on the opposite surface are almost in balance. The former rate may be controlled by the transfer of hydrate-former molecules from the film surface into the water phase, while the latter rate is presumed to be controlled by the water permeation into the film. According to this view, the hydrate funnels observed in the present experiments could be even thinner because of the presence of forced flow of water over the funnel surfaces which would enhance the film-to-water mass transfer, thereby reducing the funnel thickness at which the formation and the dissociation of hydrate crystals were in balance.

The mechanism underlying the lateral growth of a hydrate film along the liquid–liquid interface, which is seen as the growth of each hydrate funnel during each interval of drop detachment, is worth discussing here. In general, three processes are thought to be relevant to the hydrate-phase growth rate: the mass transfer to bring water and the hydrate-former molecules into contact; the kinetic process by which these molecules react to form hydrate crystals; and the heat transfer with

which the heat released at the site of hydrate-crystal formation is diffused into the surroundings (Sloan 1998). It is reasonable to assume that the kinetic process cannot be rate-controlling unless the rates of both transport processes are greatly increased (Bollavaram *et al.* 2000). In the case of hydrate-film growth along the interface, water and the hydrate-former molecules are always in contact at the site of hydrate-crystal formation, i.e. the edge of the film at which the three phases meet, and hence the mass transfer could not be the rate-controlling process for the lateral hydrate-film growth. Thus, in general agreement with Uchida, Ebinuma & Kawabata (1999) on hydrate-film growth along a water–CO_2 interface, we believe that the rate of growth of each hydrate funnel on the pendant drop surface was controlled by the heat transfer from the edge of the funnel to both the external water flow and the R-141b liquid circulating inside the drop.

In the next section, we demonstrate, using quantitative experimental data, how the formation, growth, breaking off and re-formation of a hydrate funnel succeed at a nozzle tip and how they affect the size of the drops formed successively.

4. Chronological changes in funnel length and drop diameter

The relation between the hydrate-funnel growth and the drop formation has been investigated by analysing the video record of each experimental run so that L, the axial length of the hydrate funnel, and D, the volume-equivalent spherical diameter of drops detached from the funnel, may be simultaneously plotted against t, the time lapse after the hydrate nucleation, as shown in figures 3–5. The drop diameter D was deduced from the R-141b flow rate and the instantaneous frequency of drop detachment. We focused our attention on the dependence of the hydrate-funnel/drop formation behaviour on the three system parameters – the temperature T in the test column, the velocity V_N of R-141b issuing from the nozzle, and the nozzle diameter D_N.

Figure 3 summarizes the results of experiments examining the temperature dependence of the hydrate-funnel/drop formation behaviour. Three independent runs were performed at each of the three different temperatures to determine to what extent the hydrate-funnel formation is repeatable under prescribed conditions.

At the lowest temperature, $T = 1.0\,^{\circ}\mathrm{C}$, or the largest subcooling from the hydrate/water/R-141b equilibrium temperature, $\Delta T_{\mathrm{sub}} = 7.4\,\mathrm{K}$, the rate of growth of hydrate funnels was the highest. (The apparent funnel growth rate, $\mathrm{d}L/\mathrm{d}t$, should not be confused with the rate of linear growth of hydrate films along stationary liquid–liquid interfaces (Hirai *et al.* 1999; Uchida *et al.* 1999). The former represents the excess of the actual hydrate-film growth rate over the time-averaged rate of hydrate-film loss due to periodic drop detachments.) A funnel grown to 8–10 mm in axial length L spontaneously broke, leaving a short cylindrical base on the nozzle tip. The regrowth of the funnel immediately started, at a rate nearly the same as that before it broke. The increase in D with increasing L for each hydrate funnel can readily be ascribed to the *triton* shape of the funnel (see figure 2) which indicates an increase, with increasing L, in diameter of the funnel tip from which each R-141b drop was pendent before its detachment. The gravitational force that the drops exert on the funnel increases with an increase in D or L, finally resulting in the rupture of the funnel at its waist close to the nozzle tip. The breaking of the funnel causes a sudden decrease in D to nearly the diameter of drops that would detach from the nozzle tip in the absence of any hydrate. Thus, D should exhibit a nearly periodic alternation of a gradual increase and a sudden decrease with time.

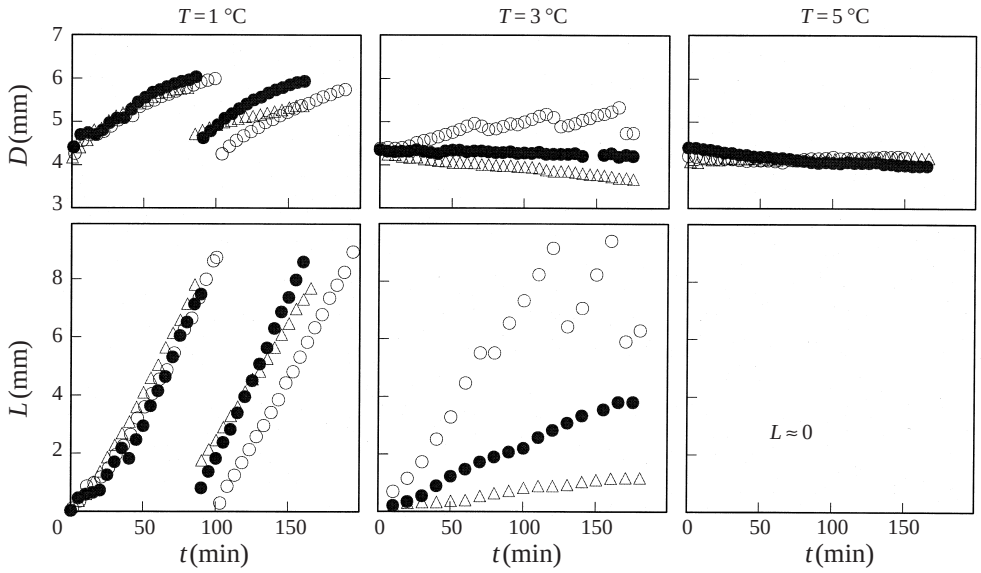

FIGURE 3. Evolution of hydrate-funnel length L and drop diameter D at three different system temperatures T. The data obtained in three different experimental runs at each T are plotted together, but with different symbols (closed circles, open circles and open triangles). Except for T, the system parameters were the same for all of the nine experimental runs, i.e. $D_N = 1.0\,\text{mm}$ and $V_N = 38\,\text{mm s}^{-1}$. Each run at $T = 1.0\,^{\circ}\text{C}$ ($\Delta T_{\text{sub}} = 7.4\,\text{K}$) was stopped when the hydrate funnel had broken twice; thus the rightmost data point indicates the length of the funnel just before its second break. In two of the three runs performed at $T = 3.0\,^{\circ}\text{C}$ ($\Delta T_{\text{sub}} = 5.4\,\text{K}$), the hydrate funnels did not break during 180 min observation periods. At $T = 5.0\,^{\circ}\text{C}$ ($\Delta T_{\text{sub}} = 3.4\,\text{K}$), hydrate funnels did not grow to a measurable length.

At a higher temperature, $T = 3.0\,^{\circ}\text{C}$ ($\Delta T_{\text{sub}} = 5.4\,\text{K}$), the behaviour of the growth and breaking of the hydrate funnels was erratic. No reproducibility was found either in $L(t)$ or in $D(t)$. Some hydrate funnels grew into the triton configuration and exhibited repetitive breaking of their leading portion, thereby causing an intermittent increase in D, but some showed a much slower growth, leading to levelling off or even a decrease in D. The slower growth of hydrate funnels through which smaller drops detached may be interpreted as follows: if a hydrate funnel happened to form as a uniform or convergent cylinder, instead of a divergent one, the frequency of drop detachment is held constant or even increased with further axial growth of the funnel. The high drop-detachment frequency thus maintained must yield a high rate of breaking off of pieces from the funnel tip, thus preventing the funnel from rapidly growing. What factor determines the initial hydrate-funnel shape is unclear at present.

At an even higher temperature, $T = 5.0\,^{\circ}\text{C}$ ($\Delta T_{\text{sub}} = 3.4\,\text{K}$), we still observed a small amount of hydrate attaching to the nozzle tip but we never found it to grow into the form of a funnel having a measurable length. Consequently, D varied only slightly throughout the observation time in each run, showing little deviation from the size of drops released from the same nozzle in the absence of any hydrate.

Figure 4 compares the results obtained at different R-141b injection velocities. At the lowest velocity, $V_N = 10\,\text{mm s}^{-1}$, the hydrate funnels broke before they grew to several millimetres in length. Because the interval of drop detachment was inevitably long at such a low R-141b velocity, an extensive hydrate film spread from the funnel

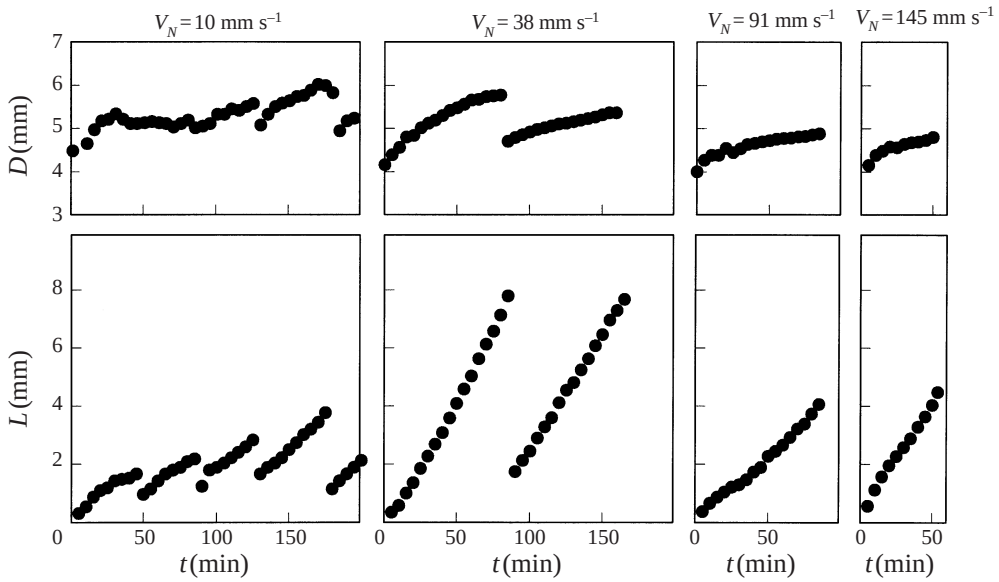

FIGURE 4. Evolution of hydrate-funnel length L and drop diameter D observed at four different V_N, the velocity of R-141b issuing from the nozzle. Other system parameters were $T = 1.0\,^{\circ}\mathrm{C}$ ($\Delta T_{\mathrm{sub}} = 7.4\,\mathrm{K}$) and $D_N = 1.0\,\mathrm{mm}$. Each of the experimental runs at $V_N = 91\,\mathrm{mm\,s^{-1}}$ and $145\,\mathrm{mm\,s^{-1}}$ had to be stopped in the course of the growth of first hydrate funnel because the R-141b initially filling the syringe-infusion pump was quickly used up.

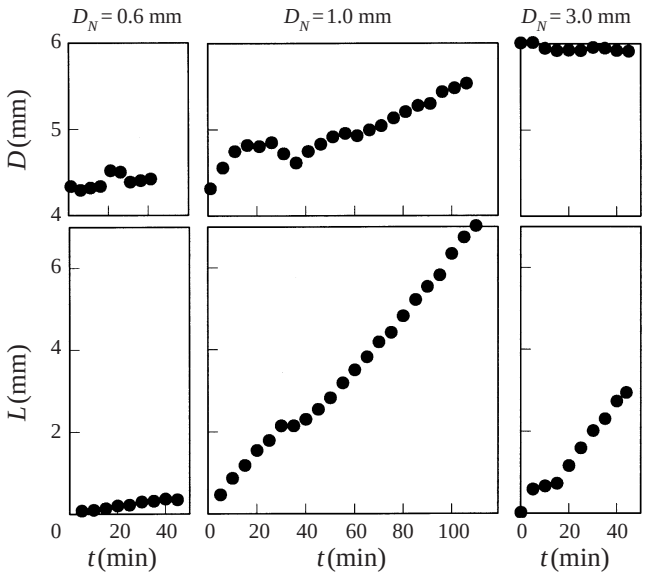

FIGURE 5. Evolution of hydrate-funnel length L and drop diameter D observed with three nozzles having different inside diameters, D_N. Other system parameters were $T = 1.0\,^{\circ}\mathrm{C}$ ($\Delta T_{\mathrm{sub}} = 7.4\,\mathrm{K}$) and $V_N = 20\,\mathrm{mm\,s^{-1}}$.

toward the frontal part of each drop before its detachment. The gravitational and inertial forces that the drop and the surrounding water exert on the hydrate film that has grown into dome-like form are easily transmitted to the funnel, thereby promoting its rupture. It was observed that an increase in V_N decreases the degree of

radial divergence of hydrate funnels, thereby providing them with longer, slenderer shapes.

Figure 5 compares the results obtained with different nozzle sizes. For the finest nozzle, $D_N = 0.6\,\text{mm}$, most of the hydrate phase grown onto the surface of each growing drop was carried away by the drop at its detachment, and hence the hydrate funnel hardly grew. The nozzle with $D_N = 1.0\,\text{mm}$ showed the most remarkable growth of the triton-shaped hydrate funnels. The thickest nozzle, $D_N = 3.0\,\text{mm}$, grew chimney-shaped funnels. The diameters of these funnels were almost unchanged along their axes and nearly the same as that of the nozzle. Consequently, D hardly changed irrespective of the axial growth of such funnels.

It seems that, in general, a hydrate funnel tends to grow to nearly fit the shape of the base portion of each drop during the intermediate, major portion of the time between successive drop detachments (for example, the stage represented by the second to fourth pictures in figure 2*a*), if the system temperature is low enough to enable a substantial extension of the funnel front over the surface of each drop before its detachment. The base portion of a drop growing at the nozzle tip has a bell shape, the opening angle of which tends to decrease with an increase in D_N or, more generally, D_N/a, where $a \equiv [\sigma/(\Delta\rho\, g)]^{1/2}$, σ being the interfacial tension between the two liquids, and $\Delta\rho$ the difference in density between the two liquids. This is presumably the reason why a chimney-like hydrate funnel formed on the thickest nozzle, hardly changing the size of drops released from the nozzle.

5. Conclusions

The experiments have revealed that the continuous injection of a hydrate-forming liquid into a continuous phase of water through a submerged nozzle causes periodic growth and breaking of a hydrate funnel on the tip of the nozzle. The funnel is constantly filled with the hydrate-forming liquid issuing out of the nozzle so that the funnel itself serves as an effective nozzle for discharging into water the hydrate-forming liquid in the form of discrete drops, each carrying hydrate fragments on its surface. A finding of potential importance from an engineering point of view is that the size of drops thus formed may periodically fluctuate synchronously with the growth and breaking of the hydrate funnel. The fluctuation in drop size may be minimized by reducing the subcooling around the nozzle from the hydrate/water/hydrate-former equilibrium temperature to prevent the hydrate funnels from appreciably growing, or by increasing the nozzle diameter so that the funnel shape is a uniform cylinder.

This paper is probably the first to report on the cyclic hydrate-funnel formation in laboratory experiments. On the other hand, we assume that this behaviour and mechanism are similar to those of the hydrate-chimney formation caused by CO_2-rich liquid emerging from the marine sediments on the sea floor, which was found a decade ago by submarine exploration (Sakai *et al.* 1990). Laboratory experiments over wider ranges of nozzle size, flow velocity through nozzles and thermodynamic conditions will help to provide a better understanding of the hydrate-former injection phenomena in a man-made or natural environment.

We thank E. Yoshimura, a former student in the Department of Mechanical Engineering, Keio University, for his assistance in preliminary experiments which preceded the work described in this paper.

REFERENCES

Akiya, T., Owa, M., Nakaiwa, M., Tanii, T., Nakazawa, K. & Ando, Y. 1991 Novel cool storage system using HCFC-141b gas clathrate. In *Proc. 26th Intersociety Energy Conversion Engineering Conference*, Vol. 6, pp. 115–119. Am. Nuclear Soc.

Aya, I, Yamane, K. & Yamada N. 1992 Stability of clathrate-hydrate of carbon dioxide in highly pressurized water. In *Fundamentals of Phase Change: Freezing, Melting, and Sublimation* (ed. P. G. Kroeger & Y. Bayazitoglu). HTD-vol. 215, pp. 17–22. ASME.

Bollavaram, P., Devarakonda, S., Selim, M. S. & Sloan, E. D., Jr 2000 Growth kinetics of single crystal sII hydrates; elimination of mass and heat transfer effects. Paper presented at *the 3rd Intl Conf. on Gas Hydrates, Salt Lake City, Utah, July 18–22, 1999*; to be published in *Ann. New York Acad. Sci.*

Brouwer, D. H., Brouwer, E. B., Maclaurin, G., Lee, M., Parks, D. & Ripmeester, J. A. 1997 Some new halogen-containing hydrate-formers for structure I and II clathrate hydrates. *Supramolecular Chem.* **8**, 361–367.

Fujioka, Y., Ozaki, M., Takeuchi, K., Shindo, Y. & Herzog, H.J. 1997 Cost comparison on various CO_2 ocean disposal options. *Energy Convers. Mgmt* **38** (Suppl.), S273–S277.

Hirai, S., Okazaki, K., Araki, N., Yoshimoto, K., Ito, H. & Hijikata, K. 1995 Experiments for dynamic behavior of carbon dioxide in deep sea. *Energy Convers. Mgmt* **36**, 471–474.

Hirai, S., Tabe, Y., Kamijo, S. & Okazaki, K. 1999 Propagation velocity of CO_2 clathrate-hydrate film. In *Greenhouse Gas Control Technologies* (ed. P. Riemer, B. Eliasson & A. Wokaun), pp. 1049–1051. Pergamon/Elsevier.

JAR Thermodynamic Tables Project Committee 1994 *JAR Thermodynamic Tables*, vol. 1 (*HFCs and HCFCs*, ver. 1.0). Japanese Association of Refrigeration, Tokyo, Japan.

Kato, M. 1998 Behavior of liquid drop formation accompanied with clathrate-hydrate formation. MSc. thesis, Graduate School of Science and Technology, Keio University, Yokohama, Japan (in Japanese).

Kumagai, A. & Takahashi, S. 1993 Saturated liquid viscosities and densities of environmentally acceptable hydrochlorofluorocarbons (HCFCs). *Intl J. Thermophys.* **14**, 339–342.

Mori, Y. H. & Mochizuki, T. 1992 Explicit expressions for volume of drops released from submerged nozzles: their derivation from semiempirical implicit correlations. *Intl J. Multiphase Flow* **18**, 141–144.

Mori, Y. H. & Mochizuki, T. 1997 Mass transport across clathrate hydrate films — a capillary permeation model. *Chem. Engng Sci.* **52**, 3613–3616.

Ohmura, R. & Mori, Y. H. 1998 Pull-out test of clathrate-hydrate films formed at water/hydrochlorofluorocarbon interfaces. *J. Mat. Sci. Lett.* **17**, 1397–1399.

Ohmura, R., Shigetomi, T. & Mori, Y. H. 1999 Formation, growth and dissociation of clathrate hydrate crystals in liquid water in contact with a hydrophobic hydrate-forming liquid. *J. Cryst. Growth* **196**, 164–173.

Ohmura, R., Shigetomi, T. & Mori, Y. H. 2000 Mechanical properties of water/hydrate-former phase boundaries and phase-separating hydrate films. Paper presented at *the 3rd Intl Conf. on Gas Hydrates, Salt Lake City, Utah, July 18–22, 1999*; to be published in *Ann. New York Acad. Sci.*

Ozaki, M., Murakami, N., Fujioka, Y., Tanii, T. & Kawata, H. 1992 Preliminary investigation on carbon-dioxide behaviour after sending into deep ocean. *Mitsubishi Juko Giho* **29**, 310–314.

PROPATH Group 1990 *PROPATH—a Program Package for Thermophysical Properties of Fluids*, ver. 7.1. Corona Publishing, Tokyo, Japan.

Ribeiro, J. & Henry, B. 1995 *Carbon Dioxide Disposal and Storage Technologies.* Institute for Prospective Technological Studies, Joint Research Centre, European Commission.

Sakai, H., Gamo, T., Kim, E.-S., Tsutsumi, M., Tanaka, T., Ishibashi, J., Wakita, H., Yamano, M. & Oomori, T. 1990 Venting of carbon dioxide-rich fluid and hydrate formation in mid-Okinawa Trough Backarc Basin. *Science* **248**, 1093–1096.

Sloan, E. D., Jr 1998 *Clathrate Hydrates of Natural Gases*, 2nd edn, Section 3.2. Marcel Dekker.

Steiner, L. & Hartland, S. 1983 Hydrodynamics of liquid–liquid spray columns. In *Handbook of Fluids in Motion* (ed. N. P. Cheremisinoff & R. Gupta), pp. 1049–1092. Butterworths.

Sugaya, M. & Mori, Y. H. 1996 Behavior of clathrate hydrate formation at the boundary of liquid water and a fluorocarbon in liquid or vapor state. *Chem. Engng Sci.* **51**, 3505–3517.

Uchida, T., Ebinuma, T. & Kawabata, J. 1999 Microscopic observations of formation processes of clathrate-hydrate films at an interface between water and carbon dioxide. *J. Cryst. Growth* **204**, 348–356.